RSC Advances

Study of Binding Interactions between MPT63 Protein and Au Nanocluster

Journal:	*RSC Advances*
Manuscript ID:	RA-ART-04-2014-003708.R3
Article Type:	Paper
Date Submitted by the Author:	31-Jul-2014
Complete List of Authors:	PATRA, AMITAVA; Indian Association for the Cultivation of Science, Materials Science Paramanik, Bipattaran; Indian Association for the Cultivation of Science, Materials Science Kundu, Amrita; CSIR-Indian Institute of Chemical Biology, Protein Folding and Dynamics Laboratory, Structural Biology and Bioinformatics Division Chattopadhyay, Krishnananda; Indian Institute of Chemical Biology, Structural Biology and Bioinformatics

Study of Binding Interactions between MPT63 Protein and Au Nanocluster

Bipattaran Paramanik,[†] Amrita Kundu,[‡] Krishnananda Chattopadhyay,[‡,*] Amitava Patra[†,*]

[†]Department of Materials Science, Indian Association for the Cultivation of Science, Kolkata 700 032, India.

[‡]Protein Folding and Dynamics Laboratory, Structural Biology and Bioinformatics Division, CSIR-Indian Institute of Chemical Biology, 4, Raja S. C. Mullick Road, Kolkata, India.

Corresponding Author

*(A.P.) E-mail: msap@iacs.res.in; Telephone: (91)-33-2473-4971; Fax: (91)-33-2473-2805.

(K.C.) E-mail: krish@iicb.res.in; Telephone: 913324995843.

Abstract

The use of protein-nanocluster conjugates in the field of bio-nanotechnology provides exciting opportunities in live cell imaging, drug delivery and detecting pathogens. Here, we have demonstrated the interactions between mycobacterium tuberculosis derived protein MPT63 and gold nanocluster (Au NC). Two single cysteine mutants of MPT63, namely G20C and G75C have been used to study the position dependence of cysteine residues on nanocluster-protein interactions. In the presence of MPT63, the enhancement of fluorescence intensity and the decay time of Au nanocluster confirm the binding of MPT63 to Au NC. The decrease in non-radiative relaxation of Au NC by solvent molecules inside the protein environment might be responsible for the increase in fluorescence intensity and decay time of Au NC. The determination of the binding constant for protein-Au NC complex reveals the difference in binding ability of wild type MPT63 and its two cysteine mutants. We have also studied the effects of pH and salt on protein-Au NC interactions. Based on these results, it is suggested that both electrostatics and other factors play crucial roles to define the complexity of protein-Au NC interactions.

Introduction

Understanding protein-nanoparticle interaction is one of the exciting fields of research at the interface of physics, chemistry and biology.[1-7] These interactions may alter protein conformation, expose novel epitopes at the protein surface, or perturb the normal protein function inducing unexpected biological reactions and toxicity.[2, 8-11] The structural changes due to binding of protein on the surface of nanoparticles have been monitored usually by infrared spectroscopy, circular dichroism, fluorescence, and NMR.[6, 8, 12, 13] Surface energy transfer (SET) has been used to understand the change of conformation of a protein and its binding site of protein molecules.[14, 15]

Metal nanoclusters are now found to be a new class of fluorescent materials which are being used to understand nano-bio interactions.[16, 17] This nanocluster has numbers of advantages like discrete electronic state, chirality, high fluorescence life time and magnetism due to strong quantum confinement.[18-20] In the case of Au NC, 6s and 5d orbitals of the Au core and 3p orbital of sulfur ligand form molecular orbitals (MOs).[21] Consequently transitions of electron from sp-sp or d-sp produce fluorescence of Au NC, which can be altered in the presence of protein.[22] Nienhaus et al.[16] have used spectroscopic techniques to study the physicochemical properties of protein upon adsorption on AuNC surface.

A number of proteins, including various types of albumins such as BSA and HSA, have been used for Au nanoparticle (NP)-protein interaction studies,[14, 23-25] because of their high abundance in blood. Covalent bonding and electrostatic interactions occur during attachment of proteins on the surface of Au NPs. In covalent bonding, surface functionalized Au NPs are attached with NH_2 or COOH groups of the protein either by coupling or direct Au-S bond formation.[26, 27] Noteworthy, thiol (S-H) has very strong interaction with Au NP or NC due to soft-soft interaction. Thus, proteins having cysteine or di-sulfide groups can be attached easily with Au NP by taking the advantage of Au and sulfur affinity.[23, 25, 28] Additionally, a typical protein contains large numbers of NH_2 and COOH groups, which would interact with Au NC via electrostatic interaction.[29] It is evident that pH and salt concentration have played a crucial role on protein-NP interactions. At lower pH, NH_2 groups and disulphide groups become protonated and as a result electron transfer or proton exchange occurs with tryptophane or tyrosine moieties of the protein.[30]

In the present work, we have used a Mycobacterium tuberculosis derived antigen MPT63 as a model protein. MPT63 is a globular protein of 130 amino acids with an immunoglobulin like fold. MPT63 has been shown to induce humoral immune response in infected guinea pigs.[31] MPT63 is a species specific protein found only in *Mycobacterium tuberculosis* and it did not show any cross reactivity towards other mycobacterium proteins. This absence of cross reactivity makes MPT63 a valuable candidate for the diagnosis of tuberculosis. We believe that, a successful Au NC-MPT63 conjugate could be useful as a potential therapeutic agent. Au NP-antibody (Ab) conjugates have already been studied by Anthony J. group.[32] They reported that the Au NP-Ab conjugate can specifically target its desired protein which can be used to monitor pathogenic infections inside human body.

X-ray crystal structure of MPT63 has already been reported at 1.5 Å resolutions (Figure 1).[33] MPT63 is a 130 amino acid β-sandwich protein. This protein consists of two halves of β-pleated sheets, one of which contains strands longer than the other one. These β-strands are anti-parallel in their orientations. MPT63 does not have any cysteine residue in its wild type (WT) sequence and we have generated two single cysteine mutants for our study. In these mutants, glycine residues at two different positions of MPT63 are replaced with cysteine residues. Two glycine residues we chose to mutate, are situated on the connecting loops of these antiparallel strands on each β-sheet. The Gly20 is situated on the longer β-sheet and Gly75 is on the shorter one. Charge distributions on the surface of these two residues are different. Gly20 is situated in more or less positively charged environment while Gly75 has a relatively neutral local environment.

Sequence and structural analysis strongly suggest that MPT63 can be included in the immunoglobulin super family. [34] In a recent study, Ghosh et al. have reported that four tryptophan residues of MPT63 show different phosphorescence characteristics due to presence of different micro-environments.[35] In the present study, our emphasis is given to understand the Au nanoclusters-MPT63 protein interactions using spectroscopic methods. We have synthesized Au NC capped by multi thiol based ligand, lipoic acid (LA). The steady state fluorescence intensity and fluorescence lifetime of Au NC are found to be increased after association with the protein. Analysis reveals that hydrophilic NH_2 and COOH groups play an important role in the binding interactions between the protein and Au NC, in addition to cysteine residues.

Experimental section

Chemicals:

Tetrachloro auric acid ($HAuCl_4$. $3H_2O$), lipoic acid (LA), were purchased from Sigma-Aldrich. Sodium borohydride ($NaBH_4$), sodium hydroxide granules (NaOH), were obtained from Merck India. Throughout the experiment high purity water (≈ 18.2 MΩ) was used. Dialysis tube (molecular cut off < 5 KDa) was purchased from Fischer-Chemicals. All the chemicals of highest purity grade were used without further purification.

Synthesis of lipoic acid capped gold nanocluster (Au NC):

Au NC was synthesized adopting the reported method, described elsewhere.[16] Briefly, 0.0026 g of lipoic acid was dispersed in 7.70 mL of water. After 5 min of vigorous stirring, 40 µL of 1(M) NaOH was added to get a clear solution of lipoic acid. 160 µL of 1wt % $HAuCl_4$ was mixed with the previous solution. After 5 min, 160 µL of previously prepared ice cool 50 mM sodium borohydride was added very leisurely. With time color of the solution became light brown to darker and stirring was continued for overnight. Red emissive Au NC were collected and dialyzed for removing unwanted reagents.

Preparation of WT and G20C, G75C MPT63:

Plasmids, bacterial strains, and site-directed mutagenesis:

The plasmid pQE30 containing the wild type MPT63 gene was kindly provided by Dr. David Eisenberg (University of California, Los Angeles, U.S.). Plasmids were transformed in E. coli XL1-Blue cells. Site-directed mutagenesis (G20C, G75C) were carried out using a Quick Change Lighting site-directed mutagenesis kit (Agilent Technologies). The mutations were verified by DNA sequencing.

Expression and purification of MPT63 and its mutants:

pQE30 was transformed into XL1-Blue cells and these transformed strains were used to express and purify wild type as well as mutants of MPT63.Single colony of transformed XL1-Blue cells were grown aerobically at 37 °C in an LB medium containing 100 µg /mL ampicillin and induced with 1 mM IPTG for 4 h when the absorbance of the medium reaches 0.5 at 600 nm. Cells were harvested by centrifugation at 8000 rpm for 10 min at 4° C and re-suspended in 40 mL of sonication buffer (50 mM Potassium phosphate, 300 mM KCl, 10 mM imidazole, pH 7.8). Cells were subjected to one cycle of freezing-thawing and 1 mM phenylmethylsulfonyl fluoride

(PMSF) was added under sonication. Cell lysates were then centrifuged at 12,500 rpm for 45 min at 4° C and supernatants were mixed with 2 mL of Ni-NTA agarose resin (Qiagen), previously equilibrated in sonication buffer, and stirred at 4° C for 1 h. The protein and resin slurry were then loaded into a column and washed with 10 volumes of sonication buffer followed by 10 volumes of wash buffer (50 mM potassium phosphate K_3PO_4, 300 mM KCl, 20 mM imidazole, pH 7.8). Protein was eluted in the same buffer with a gradient of 20 to 500 mM imidazole. The collected fractions were then analyzed by SDS-PAGE. Protein containing fractions were pooled and dialyzed overnight against ResourceQ start buffer (30mM Tris-HCl, pH 8.7). This dialyzed sample was then applied to a Resource Q FPLC column pre-equilibrated in Resource Q start buffer (30 mM Tris-HCl, 100 mM KCl, pH 8.7). The column was washed with 20 volumes of the same buffer, and the protein was eluted with a 0 to 500 mM KCl gradient. Fractions containing purified protein as assessed by SDS-PAGE (purity >90%), were pooled and dialyzed against 20 mM Sodium phosphate buffer pH 7.5 and aliquots were stored at −20 °C until required. For purification of the cysteine mutants, 10 mM DTT has been added in the protein solution. Before the experimental study, excess DTT has been removed by extensive dialysis.

Characterization

The transmission electron microscopy (TEM) image was obtained using JEOL-JEM-2100F transmission electron microscope. Sample of AuNC was drop casted on carbon coated cupper grid and used for TEM study. Room-temperature optical absorption spectra were recorded by UV-VIS spectrophotometer (Shimadzu, UV-2450) using a cuvette of 1 cm path length. The fluorescence emission spectra of all samples were obtained with FluoroMax-P (HORIBA JobinYvon) luminescence spectrophotometer upon excitation at 375 nm using 350 nM Au NC with increasing amount (50 nM to 40 μM) of protein. Additionally, the fluorescence lifetime of all samples was measured in saturating concentration of protein using decay acquisition mode of the same instrument. CD spectroscopic data were taken using a Jasco J720 spectropolarimeter (Japan Spectroscopic Ltd.). Far-UV CD spectra (between 200 and 250 nm) were recorded using 10 μM protein with a cuvette of 1 mm path length. All samples were prepared in 20 mM phosphate buffer pH 7.5 at 25^0C.

Results and discussion

Lipoic acid (LA), a multithiol based ligand is chosen as the capping agent for Au NC synthesis due to the strong sulfur-gold interaction.[16, 21, 25, 28, 36, 37] Figure 2 shows the TEM image of as synthesized NC, indicating highly mono dispersed particles formation with an average size of 1.6 nm. Noteworthy, particles of gold having typical size less than 2 nm are considered Au NC, having distinct transition from highest occupied molecular orbital (HOMO) to lowest unoccupied molecular orbital (LUMO).[38, 39] As TEM images (low and high resolution TEM images of Au NC are represent in figure S1 in the supporting information) suggest that the sizes of the as synthesized particles are about 1.6 nm then particles are Au NC, and not Au NP. In addition, UV-vis spectrum of the synthesized particles (blue curve of figure 3) shows no absorption at 520 nm, a well-known characteristic of surface plasmon resonance (SPR) of Au NP. Rather, an absorption shoulder at 280-400 nm has been observed (Figure 3), which is the characteristic of molecule like distinct d-sp, sp-sp transition of the Au NC.[16] Thus, the absence of SPR further supports the formation of Au nanoclusters. Figure 3 (represented by red curve) shows strong fluorescence spectra of synthesized Au NC with the emission maxima at 689 nm, which is observed upon excitation at 375 nm. The near-infra red (IR) emission of the particles also supports the HOMO-LUMO transition of the NC. However, the emission of the Au NC not only arises from HOMO-LUMO transition but also from ligand to metal charge transfer (LMCT) transition.[22] Decay time of Au clusters has been measured to understand photophysical behavior. The average decay time of AuNC (figure S2) is 2.87 μs, which is much longer than normal QDs or conventional dyes. The longer decay time of Au NC arises due to LMCT via Au-S bonds.[22] Like BSA capped Au NC, direct electron donation between electron rich oxygen atoms of the LA and the Au core may also be responsible for the longer decay time of the NC, as anticipated by Jin et al.[22]

CD spectroscopic study

Far-UV CD is an important tool to evaluate the change in the secondary structure of a protein in the presence of foreign additives like surfactants, acids, bases, salts or nanoparticles. The change of β-sheet and helical structure or unfolding of a protein is a very common phenomenon in the presence of NP or NC.[40-42] CD spectroscopy has been performed to elucidate the structural information in this immunoglobulin protein in the absence and presence of Au NC.

Figure 4A shows the far-UV CD spectrum of MPT63 (wild type, MPT63G75C and MPT63G20C) which is characterized by a prominent negative peak at 216 nm, confirming its overall beta sheet secondary structure. [33] The far-UV CD spectrum also shows another peak at 231 nm. Although the exact reason for the presence of 231 nm peak is not known, it has been hypothesized that the tertiary interaction of the aromatic residues inside the hydrophobic core of the protein may be responsible. [43] It may be noted that similar peaks at this region have been observed in the case of other proteins with immunoglobulin like folds. [44] Far UV CD spectra in presence and absence of Au NC of WT MPT63 protein is depicted in the inset of fig. 4A. On the other hand, the CD spectra in absence and presence of Au NC for other proteins (MPT63G75C and MPT63G20C) are demonstrated in fig. S4 (supporting information). For all proteins, the ellipticity decreases in presence of Au NC. However, the overall profile and characteristic of the far UV CD spectra remain very similar in the absence and presence of Au NC. Figure 4B shows a typical steady state fluorescence emission spectrum of WT MPT63 which is obtained upon excitation at 295 nm. The emission maximum is obtained at 328 nm, which is typical of a folded globular protein. The far-UV CD as well as the fluorescence emission spectra of both cysteine mutants of MPT63 (G20C and G75C) are similar to that of the wild type protein (Figures 4A and 4B), suggesting similar secondary structure for the folded states of these proteins.

Binding interaction and decay time enhancement

Figure 5A shows the respective fluorescence spectra of Au NC in the presence of wild type (WT) and cysteine mutant two MPT63 proteins. A significant increase in fluorescence intensity is observed after proteins addition to Au NC. The fluorescence intensity of Au NC with saturating concentration of proteins (WT MPT63 and cysteine mutant proteins) is plotted in figure 5B. The fluorescence intensity of G20C is significantly higher than G75C and wild type MPT63. To evaluate the binding constant of the protein-Au NC complex, all the data have been fit to the following equation [16]

$$F = F_0 + (F_{max} - F_0)/ [1+ (K_D / [protein])^n] \quad (1)$$

where, F_0 and F are the fluorescence intensities of Au NCs in the absence and presence of proteins, respectively. F_{max} is the maximum fluorescence intensity. K_D is the equilibrium dissociation coefficient of protein-Au NC complex and n is the Hill coefficient. K_D measures binding ability of a protein-NP system, and the higher value of K_D lower the binding strength.

On the other hand, the Hill coefficient is generally measured the co-operativity. Table 1 shows the values of K_D and n obtained for different proteins in different pH s' and salt. As evident in Table 1, K_D value of wild type MPT63 is 7.2 where there is no cysteine residue. The values of K_D are 5.3 and 6.8 for G20C and G75C protein, respectively. The lowest K_D for G20C mutant suggests the strongest binding between Au NC and G20C. For WT and both the cysteine mutants, the values of n are found to be approximately 1. It can be noted that the n value for the binding between HSA and LA capped Au NC was also found around 1.[16] In contrast, the n value for the binding between Au NC and lysozyme or ApoE4 is above 2, suggesting greater co-operativity.

It is suggested that the enhancement of fluorescence intensity is due to the binding of the protein to the highly surface active Au NC. A large number of amine and carboxylic groups may assist the binding interactions between the protein and Au NC.[22, 45] Thus, Au NC surface is surrounded by protein molecules, which prevents direct contact of water molecules from the Au NC surface and enhance the emission intensity because water causes the non-radiative relaxation.[46] To get further insight into this, we have measured the decay time of Au NC in the presence of saturating concentration of wild type (WT) and cysteine mutant MPT63 proteins. The decay time measurements support the result obtained from the steady state fluorescence study. The decay time of Au NC is found to be the highest (5.03 μs) for the G20C mutant (figure S2) in phosphate buffer. In contrast, the decay time values are 4.14 μs and 4.73 μs for Au NC-protein complexes of WT and G75C, respectively (Table 1 and figure S2). The enhancement of decay time for protein-Au NC complex compared to bare Au NC (2.87 μs) confirms the less non-radiative relaxation, which is consistent with previous report.[16] In addition, the amine and carboxylate groups in the protein are responsible for the enhancement of decay time.[22]

Effect of pH on protein-NC interactions

It is known that pH influences the protein-NP interactions due to pH dependent structural deformation of the protein as well as NP. At lower pH, amine and carboxylate groups of the protein get protonated and the protein become highly positively charged which influences the protein-NP interactions. Shang et al,[16] have already reported the strong pH dependence BSA-Au NP interactions. In this work, we have studied the pH dependence of MPT63-Au NC complex at three different pHs; in acidic pH (pH 4.0), biological pH (pH 7.5) and alkaline pH (pH 8.5) and

the data are shown in Figure 6. At saturating concentration of protein, the fluorescence intensity of Au NC-MPT63 complex is significantly higher in the case of pH 7.5, compared to that observed in the case of pH 4.0 and pH 8.5 (fig. 6A). In addition, the increases in fluorescence intensity with increasing concentration of protein at these three pH values are shown in Figure 6B. The values of n and K_D obtained by fitting the Hill equation (Equation 1) are also shown in Table 1. It can be noted that the fluorescence intensity is very weak at pH 4.0, and we cannot calculate the n and K_D, indicating weak binding with protein. At pH 4, carboxylate groups of LA become protonated (COO^- is converted to COOH) and facilitate strong H-bonding interactions between carbonyl (C=O) and acidic hydrogen (O-H) of LA. This strong hydrogen bonding causes the aggregation of Au NC which is further confirmed by TEM study (fig. S4). The aggregation of Au cluster is the reason for weak fluorescence intensity. Weak binding of Au cluster with protein may be due to less surface area of aggregated Au cluster at pH 4.0. Another reason is the surface charge, both Au NC and the protein are positively charged (isoelectric point of the protein is 4.61) at pH 4.0 which causes weak binding. It is to be noted that there is no change in conformation of protein at pH 4.0 (from far- UV CD study). Thus, we can rule out the possibility of weak binding due to change of conformation.

Effect of Salt on protein-NC interactions

It is well known that inhibition of electrostatic interaction occurs at high salt concentration.[46] In our case, at 100 mM NaCl concentration, the anions of protein and nanoparticle are stabilized by the sodium counter ion and the cation of protein is stabilized by the chloride counter ion. Thus, high salt concentration reduces the ionic interaction between the protein and nanoparticle. Beside ionic interaction, various non-ionic interactions also play important roles in the formation of protein-NP corona.[2] To find the non-ionic interaction responsible in the Au NC-MPT63 complex formation, high salt concentration (100 mM NaCl) was added to the system. The corresponding data in absence and presence of 100 mM salt are also shown in Figure 7. In presence of high salt concentration slight decrease in fluorescence intensity of Au NC is observed and a very little change in the binding constant is observed (Table 1). The decay time of Au NC for Au NC-G20C complex is 5.03 μs, which decreases to 4.45 μs (figure S2) in the presence of 100 mM NaCl.

The present paper demonstrates a number of interesting findings: first, the nature of binding varies with the position of the cysteine residue and second, electrostatics seems to have a prominent role to play in the binding interaction. The results point out that, other amino acids, and not only the cysteines, may help to stabilize the protein-Au NC complex. It is seen from fig. 8 that the charge distribution around the cystein 20 is different which have strong influence on electrostatic interaction. Noteworthy, the surface charge distribution of cysteine at the 20^{th} residue is more negative (-1) compared to that at the 75^{th} residue (0). The role of electrostatic interaction on the bio-nanoparticle research has been well established. For example, electrostatic deposition of oppositely charged molecules like negatively charged DNA on gold nanoparticle surface has been reported.[47] Electrostatic layer by layer adsorption in forming multilayer proteins film had been observed by Lvov group.[48] The effect of electrostatics on the local environment of a cysteine residue has been further substantiated by Aubin-Tam et al.[26] As suggested by Wang et al.[49], the interaction between the protein and Au NC may contain several steps. In the absence of cysteine, the initial binding could be rapid and reversible and primarily guided by the solution electrostatics. The presence of cysteine provides a "hardening step", which makes the binding essentially irreversible.[49]

MPT63 is a unique protein secreted by *Mycobacterium tuberculosis* and reported immunogenic. With the help of conjugate vaccine system, MPT63 could be used as an efficient therapeutic agent. The conjugate vaccines have been extensively studied since the first glycol-conjugate vaccine for Haemophilus influenza type b (Hib), which was licensed for human.[50] Au NCs conjugated with hyaluronic acid had been reported to successfully bind and liberate anticancer drugs.[51] The position dependence observed in the present study may have further relevance. This is because, the position of the bound drug with respect to a nanocluster may be important for the overall stability as well as delivery of the drug to its target. For example, the position of the dominant epitope with respect to the carrier protein has already been shown to play crucial role in the antigen processing.[52]

Conclusion

Fluorescent Au NC has been used as a probe to monitor protein-Au NC interaction. Our results suggest that WT and two mutants of MPT63 have interacted with Au NC. The K_D and n value imply a strong and cooperative binding between the protein and Au NC. In presence of

protein, fluorescence intensity as well as decay time of Au NCs are increased due to the shielding of Au NC surface by the bound protein molecules. The present results suggest that the electrostatic and non-covalent interactions, in addition to the presence of cysteine, play important role to stabilize the protein-nanocluster interaction.

Acknowledgement

BP and AK have contributed equally to this work. SERB (DST) and "DAE-SRC Outstanding Investigator Award" are gratefully acknowledged for financial support. CSIR network project grant, HOPE, has been acknowledged. BP thanks CSIR and AK thanks UGC for awarding fellowship.

† Electronic Supplementary Information (ESI) available: TEM images of Au NC at high and low resolution, decay time of Au NC, far UV-CD spectra of different mutant of MTP63, TEM image of Au NC at pH 4.0. See DOI: 10.1039/b000000x/

References

1. C. Boyer, X. Huang, M. R. Whittaker, V. Bulmus and T. P. Davis, *Soft Matter*, 2011, **7**, 1599-1614.
2. T. Cedervall, I. Lynch, S. Lindman, T. Berggård, E. Thulin, H. Nilsson, K. A. Dawson and S. Linse, *Proc. Natl. Acad. Sci. U. S. A.*, 2007, **104**, 2050-2055.
3. S. T. Kim, K. Saha, C. Kim and V. M. Rotello, *Acc. Chem. Res.*, 2013, **46**, 681-691.
4. R. Hong, N. O. Fischer, A. Verma, C. M. Goodman, T. Emrick and V. M. Rotello, *J. Am. Chem. Soc.*, 2004, **126**, 739-743.
5. C. K. Kim, P. Ghosh, C. Pagliuca, Z.-J. Zhu, S. Menichetti and V. M. Rotello, *J. Am. Chem. Soc.*, 2009, **13**1, 1360-1361.
6. L. Calzolai, F. Franchini, D. Gilliland and F. o. Rossi, *Nano Lett.*, 2010, **10**, 3101-3105.
7. J. E. Gagner, S. Shrivastava, X. Qian, J. S. Dordick and R. W. Siegel, *J. Phys. Chem. Lett.*, 2012, **3**, 3149-3158.
8. J. J. Gray, *Curr. Opin. Struct. Biol.*, 2004, **14**, 110-115.
9. A. Mukhopadhyay, N. Joshi, K. Chattopadhyay and G. De, *ACS Appl. Mater. Interfaces*, 2011, **4**, 142-149.
10. N. Joshi, A. Mukhopadhyay, S. Basak, G. De and K. Chattopadhyay, *Part. Part. Syst. Charact.*, 2013, **30**, 683-694.
11. X. Michalet, F. F. Pinaud, L. A. Bentolila, J. M. Tsay, S. Doose, J. J. Li, G. Sundaresan, A. M. Wu, S. S. Gambhir and S. Weiss, *Science*, 2005, **307**, 538-544.
12. S. Sharma, S. Sarkar, S. Paul Simanta, K. Chattopadhyay and S. Roy, *Sci. Rep.*, 2013, **3**, 3525.
13. S. M. Lystvet, S. Volden, O. Halskau and W. R. Glomm, *Soft Matter*, 2011, **7**, 11501-11509.
14. T. Sen, S. Mandal, S. Haldar, K. Chattopadhyay and A. Patra, *J. Phys. Chem. C*, 2011, **115**, 24037-24044.
15. T. Sen, K. K. Haldar and A. Patra, *J. Phys. Chem. C*, 2008, **112**, 17945-17951.
16. L. Shang, S. Brandholt, F. Stockmar, V. Trouillet, M. Bruns and G. U. Nienhaus, *Small*, 2012, **8**, 661-665.

17. X. Liu, F. Wang, R. Aizen, O. Yehezkeli and I. Willner, *J. Am. Chem. Soc.*, 2013, **135**, 11832-11839.
18. H. Qian, M. Zhu, Z. Wu and R. Jin, *Acc. Chem. Res.*, 2012, **45**, 1470-1479.
19. R. Jin, *Nanoscale*, 2010, **2**, 343-362.
20. J. Zheng, C. Zhang and R. M. Dickson, *Phys. Rev. Lett.*, 2004, **93**, 077402/077401-077402/077404.
21. F. Aldeek, M. A. H. Muhammed, G. Palui, N. Zhan and H. Mattoussi, *ACS Nano*, 2013, **7**, 2509-2521.
22. Z. Wu and R. Jin, *Nano Lett.*, 2010, **10**, 2568-2573.
23. L. Shang, Y. Wang, J. Jiang and S. Dong, *Langmuir*, 2007, **23**, 2714-2721.
24. A. Wang, K. Vangala, T. Vo, D. Zhang and N. C. Fitzkee, *J. Phys. Chem. C*, 2014,**118**, 8134-8142.
25. S. H. D. P. Lacerda, J. J. Park, C. Meuse, D. Pristinski, M. L. Becker, A. Karim and J. F. Douglas, *ACS Nano*, 2009, **4**, 365-379.
26. M.-E. Aubin-Tam and K. Hamad-Schifferli, *Langmuir*, 2005, **21**, 12080-12084.
27. Q. Mu, G. Jiang, L. Chen, H. Zhou, D. Fourches, A. Tropsha and B. Yan, *Chem. Rev.*, 2014, **DOI:** 10.1021/cr400295a.
28. C.-A. J. Lin, T.-Y. Yang, C.-H. Lee, S. H. Huang, R. A. Sperling, M. Zanella, J. K. Li, J.-L. Shen, H.-H. Wang, H.-I. Yeh, W. J. Parak and W. H. Chang, *ACS Nano*, 2009, **3**, 395-401.
29. H. Bayraktar, S. Srivastava, C.-C. You, V. M. Rotello and M. J. Knapp, *Soft Matter*, 2008, **4**, 751-756.
30. *Principles of fluorescence spectroscopy, 3rd Edition, Joseph R. Lakowicz, editor*, 2008.
31. C. Manca, K. Lyashchenko, H. G. Wiker, D. Usai, R. Colangeli and M. L. Gennaro, *Infect. Immun.*, 1997, **65**, 16-23.
32. A. J. Di Pasqua, R. E. Mishler Ii, Y.-L. Ship, J. C. Dabrowiak and T. Asefa, *Mater. Lett.*, 2009, **63**, 1876-1879.
33. C. W. Goulding, A. Parseghian, M. R. Sawaya, D. Cascio, M. I. Apostol, M. L. Gennaro and D. Eisenberg, *Protein Sci.*, 2002, **11**, 2887-2893.

34. D. M. Halaby and J. P. E. Mornon, *J. Mol. Evol.*, 1998, **46**, 389-400.
35. R. Ghosh, M. Mukherjee, K. Chattopadhyay and S. Ghosh, *J. Phys. Chem. B*, 2012, **116**, 12489-12500.
36. X. Dou, X. Yuan, Y. Yu, Z. Luo, Q. Yao, D. T. Leong and J. Xie, *Nanoscale*, 2014, **6**, 157-161.
37. Y. Yu, Q. Yao, Z. Luo, X. Yuan, J. Y. Lee and J. Xie, *Nanoscale*, 2013, **5**, 4606-4620.
38. Y. Negishi, K. Nobusada and T. Tsukuda, *J. Am. Chem. Soc.*, 2005, **127**, 5261-5270.
39. M. Zhu, C. M. Aikens, F. J. Hollander, G. C. Schatz and R. Jin, *J. Am. Chem. Soc.*, 2008, **130**, 5883-5885.
40. J. Xie, Y. Zheng and J. Y. Ying, *J. Am. Chem. Soc.*, 2009, **131**, 888-889.
41. J. S. Mohanty, P. L. Xavier, K. Chaudhari, M. S. Bootharaju, N. Goswami, S. K. Pal and T. Pradeep, *Nanoscale*, 2012, **4**, 4255-4262.
42. B. Paramanik, S. Bhattacharyya and A. Patra, *Chem. Eur. J.*, 2013, **19**, 5980-5987.
43. A. L. Rucker, C. T. Pager, M. N. Campbell, J. E. Qualls and T. P. Creamer, *Proteins: Struct., Funct., Bioinf.*, 2003, **53**, 68-75.
44. S. Vuilleumier, J. Sancho, R. Loewenthal and A. R. Fersht, *Biochemistry*, 1993, **32**, 10303-10313.
45. S. Gomez, K. Philippot, V. Colliere, B. Chaudret, F. Senocq and P. Lecante, *Chem. Commun.*, 2000, 1945-1946.
46. M.-C. Daniel, I. B. Tsvetkova, Z. T. Quinkert, A. Murali, M. De, V. M. Rotello, C. C. Kao and B. Dragnea, *ACS Nano*, 2010, **4**, 3853-3860.
47. M. G. Warner and J. E. Hutchison, *Nat. Mater*, 2003, **2**, 272-277.
48. Y. Lvov, K. Ariga, I. Ichinose and T. Kunitake, *J. Am. Chem. Soc.*, 1995, **117**, 6117-6123.
49. A. Wang, K. Vangala, T. Vo, D. Zhang and N. C. Fitzkee, *J. Phys. Chem. C*, 2014, **118**, 8134-8142.
50. D. Goldblatt, Clin. Exp. Immunol., 2000, **119**, 1-3.
51. N. Li, Y. Chen, Y.-M. Zhang, Y. Yang, Y. Su, J.-T. Chen and Y. Liu, *Sci. Rep.*, 2014, **4**, 4164.

52. M. Ghosh, A. K. Solanki, K. Roy, R. R. Dhoke, Ashish and S. Roy, Vaccine, 2013, **31**, 4682.

Figure captions:

Table 1: N and K_D values of protein-AuNC systems.

Figure 1. Crystal structure of MPT63 with the positions of two glycine residues at 20st and 75th positions.

Figure 2. TEM image of lipoic acid capped AuNC.

Figure 3. Absorption (a) and emission (b) spectrum of lipoic acid capped AuNC.

Figure 4. A) Far-UV CD spectra of MPT63G75C (a), wild type MPT63G (b) and MPT63G20C protein (c). B) Fluorescence emission spectra of MPT63G75C (a), MPT63G20C (b) and wild type MPT63 (c) proteins at room temperature in 20 mM sodium phosphate buffer pH7.5. The far UV-CD spectra of WT MPT63 in the absence (red) and presence (black) of AuNC are shown in the inset of Figure 4A.

Figure 5. A) Fluorescence emission spectra of (a) only AuNC and in saturating concentration of (b) WT MPT63, (c) MPT63G75C and (d) MPT63G20C. B) Fluorescence intensity of AuNC is plotted against variable concentration of proteins; (a) MPT63G20C, (b) MPT63G75C and (c) wild type MPT63 .The red lines represent fits to the equation 1.

Figure 6. A) Fluorescence emission spectra of AuNC-MPT63G20C complex at (a) pH 7.5, (b) pH 8.5 and (c) pH 4.0. B) Fluorescence intensity of AuNC is plotted against MPT63G20C protein concentration at (a) pH 7.5 and (b) pH 8.5.The red lines represent fits to the equation 1.

Figure 7. A) Fluorescence emission spectra of AuNC-MPT63G20C complex in the (a) absence and (b) presence of salt. B) Fluorescence intensity of AuNC is plotted against MPT63G20C protein concentration in absence (a) and in presence (b) of 100 mM NaCl. The red lines represent fits to the equation 1.

Figure 8. Charge distribution around 5Å area of a) 20th and b) 75th residues (in pink) of MPT63. Red, blue and white colors represent negative, positive and neutral changes, respectively.

Table 1: N and K_D values of protein-Au NC systems.

Proteins	**N**	**K_D (µM)**	**Decay time (µs)**
MPT63G20C pH 7.5	1.2 ± 0.1	5.10 ± 0.5	5.19
MPT63G75C pH 7.5	1.22 ± 0.2	6.76 ± 1.1	4.73
MPT63WT pH 7.5	1.2 ± 0.2	7.18 ± 1.1	4.14
MPT63G20C with NaCl	1.27 ± 0.2	5.02 ± 0.8	4.45
MPT63G20C pH 8.5	1.16 ± 0.2	7.75 ± 1.4	-------

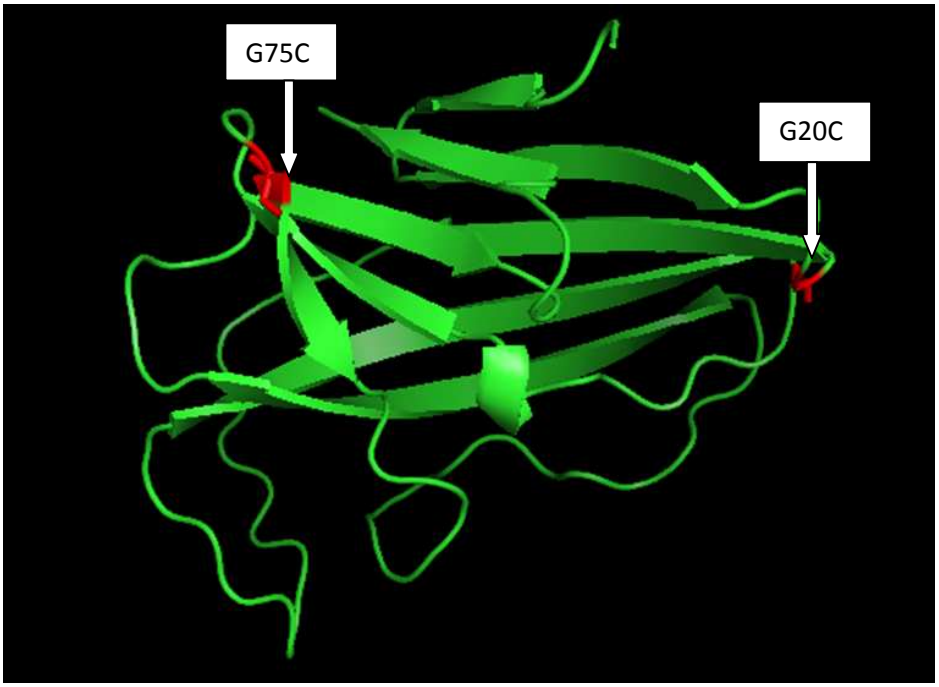

Figure 1. Crystal structure of MPT63 with the positions of two glycine residues at 20st and 75th positions.

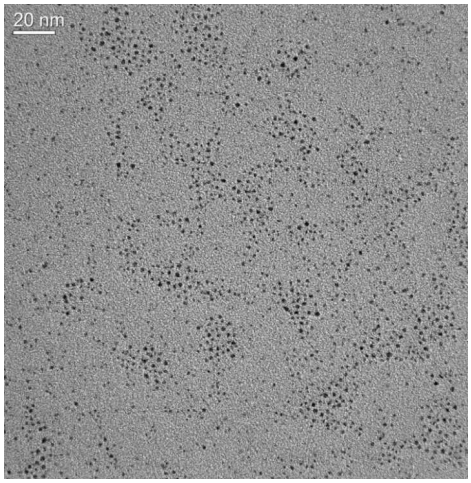

Figure 2. TEM image of lipoic acid capped AuNC.

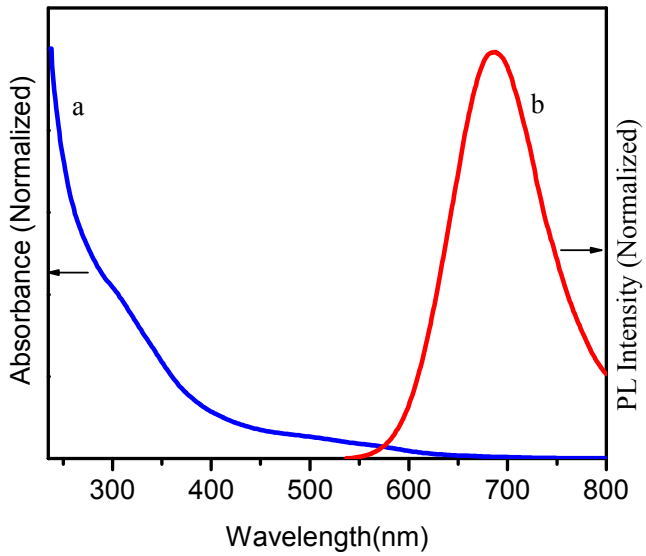

Figure 3. Absorption (a) and emission (b) spectrum of lipoic acid capped AuNC.

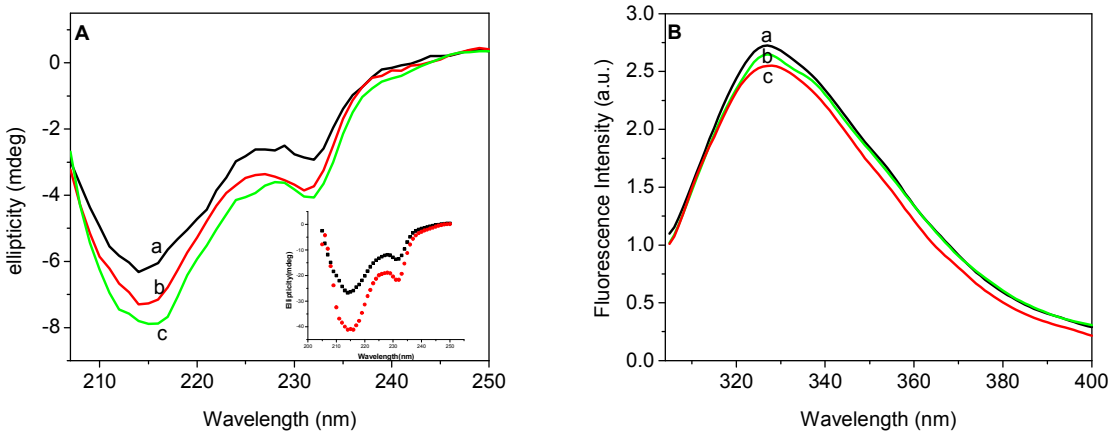

Figure 4. A) Far-UV CD spectra of MPT63G75C (a), wild type MPT63G (b) and MPT63G20C protein (c). B) Fluorescence emission spectra of MPT63G75C (a), MPT63G20C (b) and wild type MPT63 (c) proteins at room temperature in 20 mM sodium phosphate buffer pH7.5. The far UV-CD spectra of WT MPT63 in the absence (red) and presence (black) of AuNC are shown in the inset of Figure 4A.

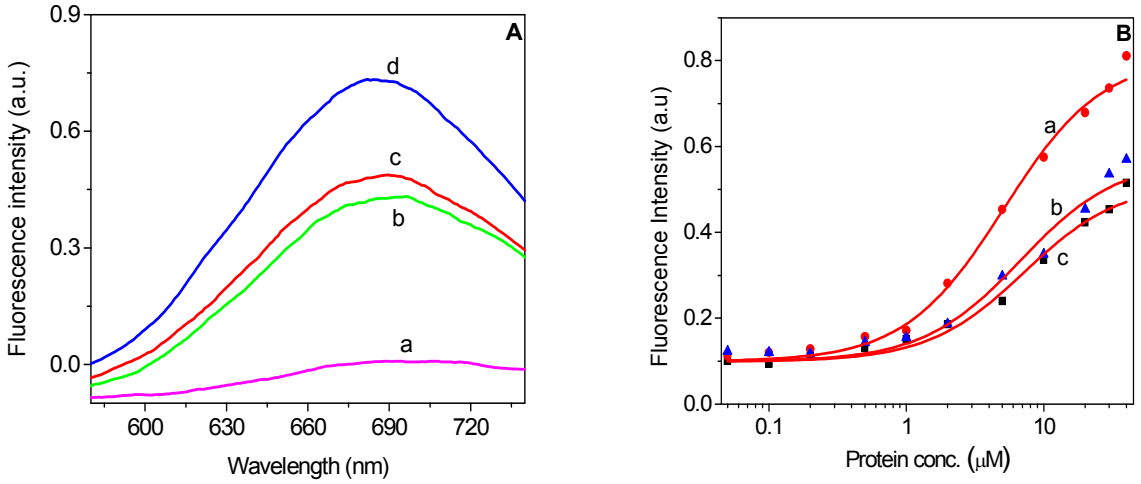

Figure 5. A) Fluorescence emission spectra of (a) only AuNC and in saturating concentration of (b) WT MPT63, (c) MPT63G75C and (d) MPT63G20C. B) Fluorescence intensity of AuNC is plotted against variable concentration of proteins; (a) MPT63G20C, (b) MPT63G75C and (c) wild type MPT63 .The red lines represent fits to the equation 1.

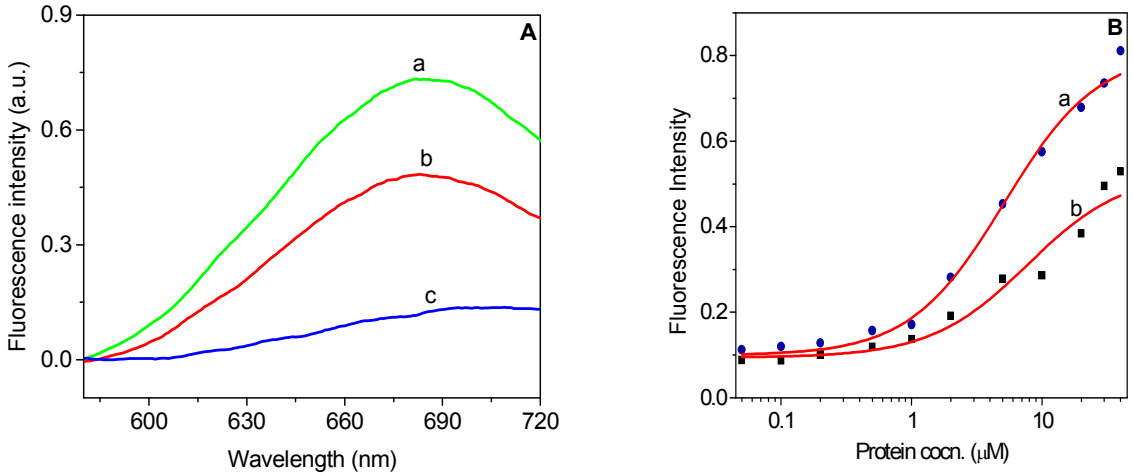

Figure 6. A) Fluorescence emission spectra of AuNC-MPT63G20C complex at (a) pH 7.5, (b) pH 8.5 and (c) pH 4.0. B) Fluorescence intensity of AuNC is plotted against MPT63G20C protein concentration at (a) pH 7.5 and (b) pH 8.5.The red lines represent fits to the equation 1.

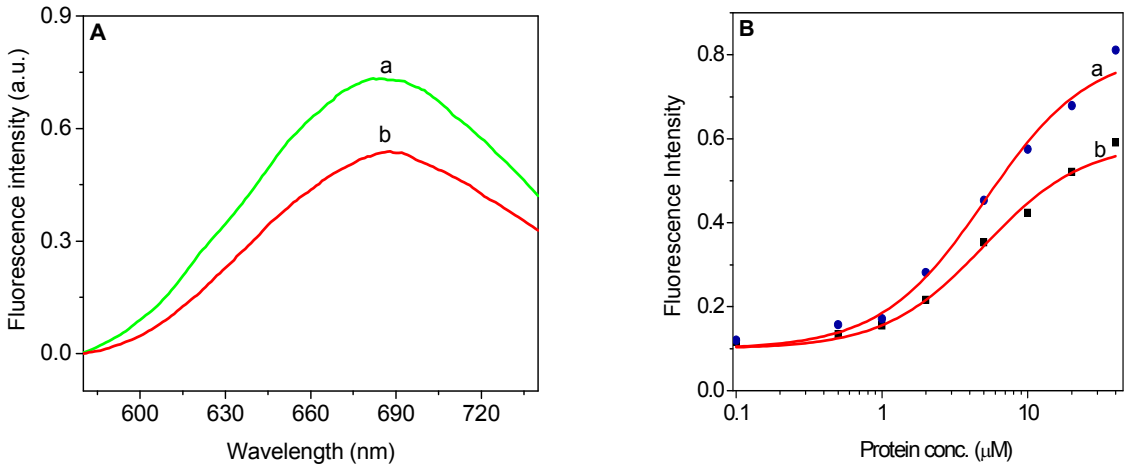

Figure 7. A) Fluorescence emission spectra of AuNC-MPT63G20C complex in the (a) absence and (b) presence of salt. B) Fluorescence intensity of AuNC is plotted against MPT63G20C protein concentration in absence (a) and in presence (b) of 100 mM NaCl. The red lines represent fits to the equation 1.

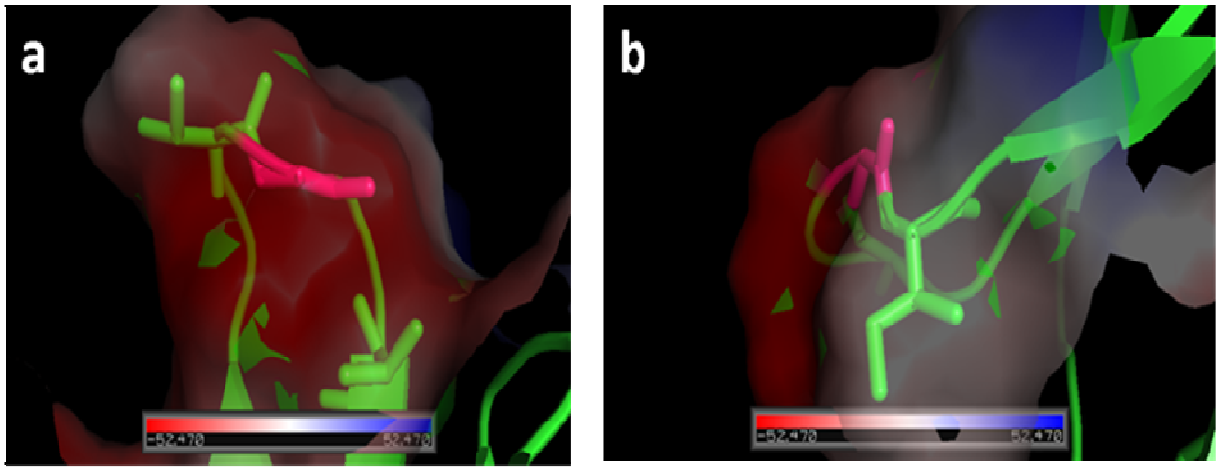

Figure 8. Charge distribution around 5Å area of a) 20th and b) 75th residues (in pink) of MPT63. Red, blue and white colors represent negative, positive and neutral changes, respectively.

TOC: Binding between AuNC and Mycobacterium Tuberculosis Derived Protein.